HHS Public Access

Author manuscript

Nat Med. Author manuscript; available in PMC 2011 May 01.

Published in final edited form as:

Nat Med. 2010 November ; 16(11): 1321–1327. doi:10.1038/nm.2246.

The *TLX1* oncogene drives aneuploidy in T-cell transformation

Kim De Keersmaecker[1,2,3,*], **Pedro Jose Real**[1,*,†], **Giusy Della Gatta**[1,*], **Teresa Palomero**[1,4], **Maria Luisa Sulis**[1,5], **Valeria Tosello**[1], **Pieter Van Vlierberghe**[1], **Kelly Barnes**[1], **Mireia Castillo**[4], **Xavier Sole**[6,7], **Michael Hadler**[1], **Jack Lenz**[8], **Peter D. Aplan**[9], **Michelle Kelliher**[10], **Barbara L. Kee**[11], **Pier Paolo Pandolfi**[12], **Dietmar Kappes**[13], **Fotini Gounari**[14], **Howard Petrie**[15], **Joni Van der Meulen**[16], **Frank Speleman**[16], **Elisabeth Paietta**[17,18], **Janis Racevskis**[17,18], **Peter H. Wiernik**[17,18], **Jacob M. Rowe**[19], **Jean Soulier**[20,21], **David Avran**[20,21], **Hélène Cavé**[22], **Nicole Dastugue**[23], **Susana Raimondi**[24], **Jules P.P. Meijerink**[25], **Carlos Cordon-Cardo**[4], **Andrea Califano**[1,26], and **Adolfo A. Ferrando**[1,4,5]

[1] Institute for Cancer Genetics, Columbia University, New York, NY, USA [2] Department of Molecular and Developmental Genetics, VIB, Leuven, Belgium [3] Center for Human Genetics, K. U. Leuven, Leuven, Belgium [4] Department of Pathology, Columbia University Medical Center, New York, NY, USA [5] Department of Pediatrics, Columbia University Medical Center, New York, NY, USA [6] Biomarkers and Susceptibility Unit, Catalan Institute of Oncology, IDIBELL, L'Hospitalet, Barcelona, Spain [7] Biomedical Research Centre Network for Epidemiology and Public Health, Catalan Institute of Oncology, IDIBELL, L'Hospitalet, Barcelona, Spain [8] Department of Molecular Genetics, Albert Einstein College of Medicine, Bronx, NY, USA [9] The Genetics Branch, Center for Cancer Research, National Cancer Institute, Bethesda, MD, USA [10] Department of Cancer Biology, University of Massachusetts Medical School, Worcester, MA, USA [11] Department of Pathology, University of Chicago, Chicago, IL, USA [12] Departments of Medicine and Pathology, Beth Israel Deaconess Cancer Center, Harvard Medical School, Boston, MA, USA [13] Fox Chase Cancer Center, Philadelphia, PA, USA [14] Department of Medicine, University of Chicago, Chicago, IL, USA [15] Department of Cancer Biology, The Scripps Research Institute, Jupiter, FL, USA [16] Center for Medical Genetics, Ghent University Hospital, Ghent,

Contact Information: Adolfo A. Ferrando, Assistant Professor of Pediatrics and Pathology, Institute for Cancer Genetics, Columbia University Medical Center, 1130 St Nicholas Ave. ICRC-402A, New York, NY, 10032, Phone: 212-851-4611, FAX: 212-851-5256, af2196@columbia.edu.

*These authors contributed equally to this work

†Current address: Andalusian Stem Cell Bank, Centro de Investigacion Biomedica, Granada, Spain.

Author Contributions

KDK performed cellular, genetic and molecular characterization of *TLX1*-induced tumors and preleukemic thymocytes, identified *BCL11B* mutations in mouse and human tumors and wrote the manuscript. PJR generated the *TLX1* transgenic mice and characterized the tumor phenotype. GDG analyzed ChIP-chip data and gene expression signatures in human and mouse tumors. TP performed ChIP-chip. VT characterized mouse thymocytes. PVV and KDK analyzed array CGH data. MLS performed mouse tumor microarray analysis. KB and MH analyzed *TLX1* transgenic lines. MC performed histological and immunohistochemical studies. JL, PA, MK, BK, PP, DK and FG provided mouse tumor samples. HP provided gene expression data on normal mouse thymocytes. XS analyzed ChIP-chip data. JVM and FS analyzed *BCL11B* mutations in human T-ALL samples. SR, HC, ND, JS and DA provided cytogenetic data on human T-ALLs. EP, JR, PW and JR provided human T-ALL specimens from ECOG clinical trials. JM generated human expression profiling data and characterized human T-ALL samples. CCC supervised histological and immunohistochemical studies. AC supervised the bioinformatic data analysis. AAF designed the study, supervised research and wrote the manuscript.

Accession codes

Microarray data are available at Gene Expression Omnibus (accession numbers GSE19499 and GSE10609).

Belgium [17] Montefiore Medical Center-North Division, New York, NY, USA [18] New York Medical College, New York, NY, USA [19] Rambam Medical Center and Technion, Israel Institute of Technology, Haifa, Israel [20] APHP Hematology Laboratory and INSERM U944, Hôpital Saint-Louis, Paris, France [21] Université Paris 7-Denis Diderot, Institut Universitaire d'Hematology (IUH), Hopital Saint-Louis, Paris, France [22] AP-HP, Hôpital Robert Debré, Departement de Génétique; Université Paris 7-Denis Diderot, Paris, France [23] Laboratoire d'Hématologie, Hôpital Purpan, Toulouse, France [24] Department of Pathology, St. Jude Children's Research Hospital, Memphis, TN, USA [25] Department of Pediatric Oncology/Hematology, Erasmus MC-Sophia Children's Hospital, Rotterdam, The Netherlands [26] Joint Centers for Systems Biology, Columbia University, New York, NY, USA

Abstract

The *TLX1* transcription factor oncogene plays an important role in the pathogenesis of T-cell acute lymphoblastic leukemia (T-ALL). However, the specific mechanisms of T-cell transformation downstream of *TLX1* remain to be elucidated. Here we show that forced expression of *TLX1* in transgenic mice induces T-ALL tumors with frequent deletions and mutations in *Bcl11b*, and identify the presence of recurrent mutations and deletions in *BCL11B* in 16% of human T-ALLs. Most notably, mouse *TLX1* tumors were typically aneuploid and showed a marked defect in the activation of the mitotic checkpoint. Mechanistically, *TLX1* directly downregulates the expression of *CHEK1* and additional mitotic control genes and induces loss of the mitotic checkpoint in non transformed preleukemic thymocytes. These results identify a novel mechanism contributing to chromosomal missegregation and aneuploidy active at the earliest stages of tumor development in the pathogenesis of cancer.

T-ALL is an aggressive hematologic tumor resulting from the malignant transformation of T-cell progenitors. The *TLX1* transcription factor oncogene is translocated and aberrantly expressed in 5% to 10% of pediatric and up to 30% of adult T-ALL cases1–4. In addition, *TLX3*, a highly related TLX family member, is overexpressed as result of the t(5;14)(q35;q32) translocation in about 25% of pediatric TALLs and in 5% of adult T-ALL cases5. *TLX1* expression defines a distinct molecular group of T-ALL characterized by a differentiation block at the early cortical stage of thymocyte development2 and favorable prognosis1,2,6. Moreover, *TLX1* and *TLX3* leukemias seem to constitute a distinct oncogenic group with specific genetic alterations rarely found in non-TLX induced T-ALLs including the rearrangement of the *NUP214-ABL1* oncogene7 and mutations in the *WT1*8 and *PHF6*9 tumor suppressor genes. However, little is known about the specific mechanisms that mediate T-cell transformation downstream of *TLX1*. To address this question we have used an integrative genomic approach to characterize the transcriptional programs and oncogenic pathways active in human and mouse *TLX1*-induced leukemia.

RESULTS

T-ALL development in *TLX1* transgenic mice

In order to investigate the mechanisms of T-cell transformation driven by *TLX1*, we generated p56^{Lck}-*TLX1* transgenic mice in which the *Lck* proximal promoter drives expression of *TLX1* in T-cell progenitors10,11. *TLX1* transgenic mice from three founder lines showed accelerated mortality due to the development of lymphoid tumors with a median latency of 27, 32 or 46 weeks, respectively ($P<0.0001$) (Fig. 1a). Tumor-bearing mice showed enlarged thymi populated by immature lymphoblasts and leukemic infiltration of bone marrow and peripheral organs including lymph nodes, spleen, liver and kidneys (Fig. 1b). Overall, 92% of *TLX1* transgenic animals developed tumors at 52 weeks. *TLX1*-induced leukemias showed high levels of *TLX1* protein (Fig. 1c–d) and expression of CD3 indicative of a T-cell phenotype (Fig. 1e). Moreover, flow cytometry analysis demonstrated the expression of CD4 and CD8 in most tumors (Fig. 1f–g). In addition, this analysis revealed significant heterogeneity in these leukemias with 53% of the tumors showing two or more immunophenotypically different cell populations (Fig. 1f). Finally, *TLX1*-induced tumors showed clonal expression of a single *TCRB* chain in 4/5 tumors examined and only 2 *TCRB* chains in the remaining sample (Fig. 1h), indicating that despite their heterogeneous immunophenotypes these are monoclonal T-cell tumors.

Mouse and human *TLX*-induced T-ALLs have a common expression signature

To address the transcriptional programs activated in mouse *TLX1* leukemias, we analyzed the expression profiles of mouse tumors from *TLX1* transgenics (n=6) and of T-ALLs generated by retroviral insertional mutagenesis or arising in the context of different T-ALL transgenic and knockout models including *Tal1*, *Lmo2* and *Olig2/Bhlhb1* transgenics and *Tcf3/E2A*, *Trp53* and *Pten* knockouts (n=49) (Supplementary Table 1). Significant differentially expressed genes were calculated by Comparative Marker Selection Genepattern tool12 using t-test statistical test and non-parametric *P* value calculation (1,000 random permutations). This analysis revealed that *TLX1* tumors are characterized by a distinct gene expression signature with upregulation of 114 genes and downregulation of 377 transcripts (Fold change >2, $P<0.005$) (Fig. 2a; Supplementary Table 2). Moreover, Gene Set Enrichment Analysis (GSEA) of human T-ALL (n=82) using these mouse *TLX1*-signature genes showed significant enrichment in human *TLX1* and *TLX3* tumors ($P<0.001$) (Fig. 2b; Supplementary Table 3), highlighting the relevance of our mouse model for the analysis of *TLX*-induced transformation.

TLX1 expression blocks T-cell development and induces apoptosis

Next, we decided to explore the effects and mechanistic role of *TLX1*-expression in T-cell progenitors in young *TLX1* transgenic mice prior to the development of T-ALL. Analysis of TLX1-transgenic mice at 3 and 6 weeks of age showed a drastic reduction in thymic size and cellularity compared with littermate controls (Fig. 3a), but no clear defects in cell proliferation (Fig. 3b). Flow cytometry analysis of thymocyte differentiation markers in *TLX1* transgenic animals and littermate controls showed a defect in T-cell development with arrest at the double negative 2 (DN2) stage of thymocyte differentiation (Fig. 3c), which was accompanied by a marked increase in apoptosis (Fig. 3d,e). Consistent with these results,

transgenic expression of *BCL2* in *Lck-TLX1 VavP-BCL2* double transgenic mice abrogated apoptosis (Fig. 3f) and rescued the defect in thymus size (Fig. 3g) and cellularity (Fig. 3h) observed in preleukemic *TLX1*-transgenic mice.

Secondary mutations in the pathogenesis of *TLX1*-induced T-ALL

The prolonged latency in the development of T-ALL in *TLX1* transgenic mice and the clonal nature of these tumors prompted us to investigate the presence of cooperating mutations involved in the pathogenesis of *TLX1*-induced leukemias. Activating mutations in *NOTCH1* are present in over 50% of human T-ALLs13,14. Similarly, prototypical mutations in *Notch1* were present in 3/25 (12%) *TLX1*-induced mouse tumors (Supplementary Table 4). Moreover, array Comparative Genomic Hybridization (aCGH) analysis revealed the presence of recurrent numerical and structural chromosomal alterations in these tumors (Fig. 4a, Supplementary Fig. 1). Thus, focal homozygous deletions affecting the *Pten* tumor suppressor gene were present in 4/15 (27%) samples (Fig. 4a, Supplementary Fig. 1, Supplementary Table 5). In addition, immunohistochemical analysis of Pten showed loss of Pten protein expression in 11/24 (42%) tumors (Supplementary Fig. 1). Notably, *PTEN* deletions, mutations and loss of PTEN protein expression have been reported in 20% of human T-ALLs15,16. Chromosomal deletions involving *Trp53* and *Ikzf1*, which are sporadically mutated and deleted in human T-ALLs17,18, were detected in one tumor each (Fig. 4a, Supplementary Fig.1, Supplementary Table 5). In addition three mouse *TLX1* T-ALL samples harbored heterozygous deletions in chromosome 12 with a common deleted region containing only the *Bcl11b* gene (Fig. 4a–c, Supplementary Table 5). Moreover, DNA sequence analysis of *Bcl11b* showed the presence of *Bcl11b* mutations in 4/15 (27%) mouse *TLX1*-induced T-ALLs (Fig. 4d–e, Supplementary Table 6), which together with the 3 *Bcl11b* deletions identified in our aCGH analysis brings the prevalence of *Bcl11b* alterations in mouse *TLX1*-induced tumors to 7/15 (47%). Notably, mutation analysis of *Bcl11b* in T-ALL tumors occurring in *Pten* knockout animals (n=6), *Trp53* knockout mice (n=2), *Ctnnb1* transgenic animals (n=4) or induced by retroviral insertional mutagenesis (n=9) failed to detect any *Bcl11b* mutations in these non-*TLX1* transgenic tumors (Fisher's exact test $P < 0.001$).

Recurrent deletions and mutations in *BCL11B* in human T-ALL

Bcl11b encodes a zinc finger transcription factor with a critical role in the differentiation and survival of T-cell progenitors in the thymus19,20. Given the similarities between our mouse model of *TLX1*-induced leukemia and human T-ALL, we hypothesized that *BCL11B* alterations could also be implicated in the pathogenesis of human T-ALL. Most notably, aCGH analysis of human T-ALL samples showed the presence of focal heterozygous deletions encompassing the *BCL11B* locus in 2/69 (3%) T-ALL cases (Fig. 5a). In addition, mutation analysis of *BCL11B* in human T-ALL demonstrated the presence of truncating frameshift mutations and missense point mutations in 9/71 (13%) cases analyzed (Fig. 5b). Interestingly, all 6 *BCL11B* missense mutations involved zinc finger domains (Fig. 5b). One sample showed compound heterozygous *BCL11B* mutations while the remaining 5 cases harbored heterozygous *BCL11B* lesions (Supplementary Table 7). Notably, sequence analysis of samples obtained at the time of clinical remission demonstrated the somatic origin of *BCL11B* mutations in all 6 cases with available material (Fig. 5c). Finally,

expression analysis of *TLX1* or *TLX3* in 8 T-ALLs harboring mutations or deletions in *BCL11B* with RNA available showed aberrant expression of these transcription factor oncogenes in 5/8 (63%) [*TLX1* (4/8); *TLX3* (1/8)] of these samples (Supplementary Table 7). Altogether, these results identify *BCL11B* as a tumor suppressor gene recurrently deleted and mutated in human T-ALL.

Interaction between *BCL11B* and *TLX1* in T-cell transformation

The identification of a high prevalence of *Bcl11b* mutations and deletions in *TLX1*-induced tumors suggest a specific genetic interaction between these two genes in T-cell transformation. To test if *BCL11B* could be a direct transcriptional target of TLX1 in T-ALL, we analyzed the binding of TLX1 to the *BCL11B* promoter via chromatin immunoprecipitation analysis in ALL-SIL, a T-ALL cell line expressing high levels of *TLX1* as result of the t(10;14)(q24;q11) translocation21. This analysis revealed that indeed TLX1 binds to the *BCL11B* promoter (Fig. 5d). Moreover, siRNA knockdown of TLX1 in this cell line resulted in transcriptional upregulation of *BCL11B* (Fig. 5e), indicating that *BCL11B* is a direct transcriptional target downregulated by TLX1 in T-ALL.

TLX1 T-ALLs are aneuploid and have a defective mitotic checkpoint

In addition to identifying focal areas of amplification and deletion, our aCGH analysis of mouse *TLX1* tumors showed gains and losses of whole chromosomes in most samples analyzed, suggesting a high prevalence of numerical chromosomal abnormalities in these leukemias (Fig. 4a, Supplementary Table 8). Spectral karyotyping (SKY) analysis confirmed these results and showed the presence of trisomy 15 in 3/4 *TLX1* tumor samples analyzed (Fig. 6a, Supplementary Table 8). Overall, 78% (14/18) of *TLX1*-induced leukemias showed chromosomal gains and losses, with 67% (12/18) harboring trisomy 15 (alone or in combination with trisomy 17, gain of chromosome Y, monosomy X or hyperdiploidy) (Fig. 6b, Supplementary Table 8). Previous *in vitro* studies had associated *TLX1* with alterations in the G2/M cell cycle checkpoint22 and forced expression of *TLX1* can induce aneuploidy in B-cells after disruption of the mitotic spindle23. To test the function of the mitotic checkpoint in our *TLX1*-induced leukemias we treated TLX1-T-ALL lymphoblasts with taxol, which impairs microtubule remodeling. This analysis revealed that *TLX1* mouse T-ALL lymphoblasts fail to arrest in mitosis following disruption of the mitotic spindle (Fig. 6c). In contrast, tumors induced by the *TAL1*, *TAL1* plus *LMO1*, *TAL1* plus *LMO2* and *NUP214-ABL1* T-ALL oncogenes showed a marked accumulation of cells in mitosis after taxol treatment (Fig. 6c, Supplementary Fig. 2). Similar results were obtained using nocodazole, which disrupts tubulin polymerization (Fig. 6c), and BrdU incorporation analysis verified that *TLX1* mouse tumors proliferate and fail to arrest in M phase following disruption of the mitotic spindle (Supplementary Fig.3).

TLX1 directly downregulates mitotic genes in T-cell transformation

The acquisition of chromosomal instability may represent an early event in the pathogenesis of cancer24. To investigate the specific mechanisms involved in the earliest stages of *TLX1*-induced transformation, we performed microarray gene expression analysis of sorted preleukemic DN2 cells from 3 week old mice. Significant differentially expressed genes

were calculated by Comparative Marker Selection Genepattern tool12 as described above. This analysis revealed marked differences in gene expression in *TLX1* transgenic thymocytes and DN2 cells from normal littermate controls with 175 genes upregulated and 138 genes downregulated in *TLX1*-expressing cells (Fold change > 1.5, $P<0.005$) (Supplementary Table 9). Next, and to specifically address the role of direct TLX1 target genes in T-cell transformation, we performed ChIP-chip analysis of TLX1 in ALL-SIL cells. In these experiments, TLX1 chromatin immunoprecipitates were hybridized to human proximal promoter arrays and analyzed using ChIP-chip Significance Analysis (CSA) to identify high confidence TLX1 direct target genes25. This analysis identified 5,549 promoters bound by TLX1 with a significance cutoff of $P<0.0001$ (Supplementary Table 10). Integration of these ChIP-chip results with the gene expression signature associated with aberrant expression of *TLX1* in T-cell progenitors revealed a marked enrichment of TLX1 direct target genes involved in mitosis ($P<0.001$) (Supplementary Table 11) downregulated in TLX1-preleukemic cells (Fig.6d and Supplementary Fig. 4). Notably, these included *CHEK1*, a key regulator of the mitotic spindle checkpoint and one of the genes most consistently downregulated in both mouse and human TLX-induced leukemias (Supplementary Tables 2 and 3). Consistent with these results, TLX1-knockdown in ALL-SIL cells resulted in transcriptional upregulation of *CHEK1* (Fig.6g) and pharmacologic inhibition of CHEK1 in human TALL cell lines abrogated the activation of the mitotic checkpoint upon treatment with taxol (Supplementary Fig. 5). These results suggest a mechanistic role of TLX1 in the control of cell cycle checkpoint genes at the earliest stages of T-cell transformation.

To test if *TLX1* expression can induce a defective mitotic checkpoint phenotype in preleukemic cells we isolated viable thymocytes from *TLX1-BCL2* double transgenic mice and compared them with cells obtained from *BCL2* transgenic controls. This experiment showed a marked defect in the activation of the mitotic checkpoint after taxol treatment in *TLX1-BCL2* preleukemic cells compared with *BCL2* controls (Fig. 6h). The polyclonal/non transformed nature of *TLX1-BCL2* preleukemic cells was verified by RT-PCR analysis of *TCRB* expression (Supplementary Fig. 6). Overall, these results demonstrate that the impaired control of the mitotic checkpoint in *TLX1*-transgenic mice is an early event in tumor formation that precedes clonal selection in T-cell transformation.

Chromosomal alterations in human *TLX*-induced leukemias

Overall the results described above support a direct mechanistic role for *TLX1* in the induction of chromosomal missegregation suggesting that similar mechanisms may operate in the pathogenesis of human leukemias. Most notably, and consistent with this thesis, the *TLX1*-positive ALL-SIL cell line showed a selective defect in the mitotic checkpoint (Supplementary Fig. 2). In addition, karyotype analysis of a series of 57 well characterized pediatric T-ALLs2 demonstrated a higher frequency of aneuploid karyotypes (8/13, 62%) in *TLX1* and *TLX3* positive human T-cell tumors compared with other genetic subgroups of T-ALL (5/44, 11%) (Fisher's exact test $P<0.001$) (Supplementary Table 12). Moreover, analysis of an independent series of 229 T-ALLs showed a marked predominance of numerical chromosomal abnormalities in *TLX1* and *TLX3* positive T-ALLs (aneuploidy/pseudodiploid karyotype ratios: 6/1 for *TLX1* tumors; 10/10 for *TLX3* leukemias and 24/63

for non-*TLX* T-ALLs; Fisher's exact test $P < 0.004$ for *TLX1 vs.* non-*TLX; P* <0.05 for *TLX3 vs.* non-*TLX* and $P < 0.003$ for *TLX1/TLX3 vs.* non-*TLX*) (Supplementary Table 13).

Discussion

TLX1 plays a central role in the pathogenesis of T-ALL. However the elucidation of the specific mechanisms that mediate T-cell transformation downstream of *TLX1* has been hampered by the lack of an animal model of *TLX1*-induced T-ALL and by the lack of understanding of the direct transcriptional targets controlled by *TLX1* in human leukemia. Here we demonstrate that *TLX1* transgenic mice develop clonal immature T-cell tumors highly related to human *TLX1* and *TLX3* TALLs in their clinical presentation and gene expression signatures. The extended latency in the development of leukemia in this model and the clonal nature of *TLX1*-induced tumors suggest that *TLX1* overexpression in the thymus is not sufficient for malignant transformation of T-cell progenitor cells. This thesis is further supported by the identification of recurrent cooperating mutations and chromosomal abnormalities in mouse *TLX1*-induced leukemias. Most notably, *TLX1*-induced tumors harbored recurrent alterations in oncogenes (*Notch1*) and tumor suppressor genes (*Pten, Cdkn2a*) frequently mutated in human T-ALL13–15,26. In addition this analysis revealed the presence of recurrent mutations and deletions centered on the *Bcl11b* locus in 47% of mouse *TLX1*-induced tumors analyzed. Based on these results, we hypothesized that *BCL11B* could play a tumor suppressor role in human leukemia and identified recurrent deletions and mutations in this gene in 16% of human TALLs. Notably, most *BCL11B* alterations found in mouse *TLX1*-induced tumors and in human T-ALLs were heterozygous and loss of one copy of *Bcl11b* in mice accelerates the development of thymic lymphomas after γ-irradiation or in *Trp53* heterozygous mice without loss of the wild type *Bcl11b* allele27. Finally, ChIP and expression analysis demonstrated that *BCL11B* is a direct transcriptional target downregulated by TLX1 in T-ALL. The model that emerges from these results is that aberrant expression of TLX1 partially downregulates the *BCL11B* tumor suppressor gene during T-cell transformation and that this negative transcriptional regulatory axis is fixed and reinforced by secondary genetic alterations in the *BCL11B* locus acquired during tumor progression. Strikingly, *PHF6* and *WT1*, two additional tumor suppressor genes frequently mutated in TLX1-induced T-ALL are also among the TLX1 targets identified in our ChIP-on-chip analysis (Supplementary Table 10), suggesting that this model could also apply to these TLX1-target tumor suppressor genes.

Perhaps the most striking finding in *TLX1*-induced leukemias was the presence of a very high incidence of numerical chromosomal alterations in these tumors, indicating that alterations in the mitotic machinery could play an important role in *TLX1*-induced transformation. Consistent with this model, our results demonstrate that *TLX1*-induced T-ALLs have a defective mitotic checkpoint and fail to arrest in mitosis upon treatment with taxol or nocodazole. Moreover, this mitotic checkpoint defect is readily present in preleukemic thymocytes from *TLX1* transgenic mice, suggesting that aneuploidy represents a direct effect of *TLX1* overexpression and an early event in the genesis of mouse *TLX1*-induced tumors.

Mechanistically, analysis of TLX1 direct target genes in the context of *TLX1* preleukemic thymocytes revealed that multiple *TLX1* direct target genes involved in mitosis and chromosomal segregation are downregulated in T-cell progenitor cells isolated from *TLX1* transgenic mice. Among these, *CHEK1*, a critical checkpoint regulator, is downregulated in mouse and human TLX-induced leukemias and could have a particularly prominent role in the loss of the mitotic checkpoint downstream of TLX1. However, it would be deceiving to attribute the induction of aneuploidy by TLX1 to the dysregulation of a single gene, as multiple transcripts with prominent roles in mitosis seem to be controlled by TLX1 in T-cells. In addition, a transcription independent effect of *TLX1* in the control of cell cycle via interaction with the PP2A phosphatase has been proposed22.

Overall, our results mechanistically link the aberrant expression of *TLX1* with the development of chromosomal instability at the earliest stages of T-cell transformation and illustrate the power of integrative genomic analyses of mouse and human tumors to elucidate basic mechanisms and oncogenic pathways involved in tumor initiation and disease progression.

Methods

Transgenic mice

The human *TLX1* cDNA was amplified by PCR using *BamH*I restriction site containing primers and cDNA of the human T-cell leukemia cell line ALL-SIL as template and was cloned in the pUC1017 vector, downstream of the mouse T-cell specific $p56^{Lck}$ proximal promoter. C57BL/6J VavP-*Bcl2* transgenic mice have been described before 28,29. Animal experiments were performed under the supervision of the Columbia University Medical Center IACUC.

Gene expression profiling of mouse tumors

We profiled a cohort of 6 *TLX1* transgenic-derived TALLs and additional 49 T-cell lymphoblastic tumors from different genetic models of T-ALL (see Supplementary Table 1 for details on the genetic background of tumors analyzed). Gene-expression profiling was performed using Affymetrix Mouse Genome 430A 2.0 Array following standard procedures. Raw data is available in GEO (accession number GSE19499). Array normalization was performed by DNA-Chip-Analyzer (dChip)30. Following interarray normalization we preprocessed and analyzed the microarray data for differential expression using the Genepattern platform for microarray analysis31.

Gene expression profiling human T-ALL

Affymetrix gene expression data from pediatric T-ALL samples has been reported before (GEO accession # GSE10609)32. This series encompasses 7 *TLX1* positive cases, 23 *TLX3* positive samples and 53 other T-ALLs including 33 tumors with aberrant expression of *TAL1* and *LMO2*. Tumors with high levels of expression of *HOXA9* constitute a heterogeneous molecular group resulting from translocations involving the *HOXA* loci, aberrant expression of *CALM-AF10*, *SET-NUP214* and *MLL* fusion oncogenes and were a priory excluded from this series. Enrichment of the *TLX1* direct target genes identified by

ChIP-chip ($P < 10^{-4}$) in the *TLX1* and *TLX3* class signature was analyzed by GSEA using the signal-to-noise metric and a 1,000 permutations of the class labels.

Gene expression profiling of normal and *TLX1 transgenic* thymocytes

We isolated single cell suspensions of thymi from 3 week old wild type and *TLX1* transgenic littermates and isolated $CD4^-$ $CD8^-$ $CD44^+CD25^+$ cells on a FACS ARIA Sorter (Beckton Dickinson). We collected cells in RLT buffer (Qiagen) and extracted RNA with the RNeasy mini kit (Qiagen). We verified RNA quantity and quality on a Nanodrop spectrophotometer and an Agilent Bioanalyzer 2100, respectively. We used the Ovation RNA Amplification System V2 (NuGEN) to generate amplified cDNA, which was subsequently fragmented and labeled with the FL-Ovation cDNA Biotin Module V2 (NuGEN) and hybridized on Mouse Genome 430 2.0 Arrays (Affymetrix).

Array normalization and data analysis was performed as described above. Significant differentially expressed genes were calculated by the Comparative Marker Selection Genepattern tool using t-test statistical test with an asymptotic P value and zero permutations.

For enrichment analysis of mitotic genes controlled by *TLX1* in preleukemic cells, we first identified 155 mitotic regulators (GO:0000278~mitotic cell cycle) within the top 5,549 *TLX1* targets identified by ChIP-chip (P< 0.0001) using the DAVID (http://david.abcc.ncifcrf.gov/) Functional Annotation tool, and used this geneset to run GSEA in *TLX1* transgenic versus wild type DN2 cells test using the signal-to-noise metric and 1,000 permutations of the gene list.

Array comparative genomic hybridization (aCGH)

We performed aCGH analysis of mouse tumors using the Mouse Genome CGH 244A platform (Agilent Technologies) according to the instructions of the manufacturer. To analyze these data we used DNA Analytics 4.0 software (Agilent Technologies). For Array-CGH analysis of human T-ALLs we used SurePrint G3 Human CGH 1x1M Oligo Microarrays (Agilent Technologies). We analyzed human array CGH data with the Genomic Workbench 5.0.14 software (Agilent Technologies).

Mitotic checkpoint analysis

Integrity of the mitotic checkpoint was tested by flow cytometry analysis of cell cycle in cells treated with 1 μM taxol (Sigma) (human cell lines), 0.1 μM taxol (mouse cell lines), 100 ng ml^{-1} nocodazole (Sigma) or vehicle for 24 hours. For analysis of the mitotic checkpoint in pre-leukemic mouse cells, thymocytes from 3 week old VavP-*Bcl2* and VavP-*Bcl2*/*TLX1* transgenic littermates were cultured on OP9-DL1 cells for 24 hours followed by taxol treatment and cell cycle analysis as described above.

TLX1 ChIP-chip analysis

We performed ChIP-chip analysis of TLX1 direct target genes in the ALL-SIL T-ALL cell line using a rabbit polyclonal TLX1-specific antibody (C-18, sc-880) (Santa Cruz Biotechnology) using Agilent Human Proximal Promoter Microarrays (244K features/array)

as previously described33. We identified TLX1 direct targets via ChIP-chip Significance Analysis (CSA) as described before25.

Quantitative ChIP Analysis

Relative real-time PCR quantitation of promoter sequences was normalized to β-actin levels in chromatin immunoprecipitates performed with a TLX1-specific antibody (C-18 rabbit polyclonal antibody (sc-880), Santa Cruz Biotechnology), or an IgG antibody. Primer sequences are listed in Supplementary Table 15.

siRNA knockdown

In TLX1 siRNA knockdown experiments we electroporated ALL-SIL cells (275V, 1,000 μF) using a Genepulser MXcell electroporator (Biorad) with 200 nM of Silencer Select Negative Control #1 siRNA (Ambion, cat #4390844) or TLX1 siRNA1 (5'-GAUGGAGAGUAACCGCAGAtt-3'). Knockdown efficiency was measured by quantitative RT-PCR and Western blot.

Supplementary Material

Refer to Web version on PubMed Central for supplementary material.

Acknowledgments

This work was supported by a Blood Disease Research Project research grant from The New York Community Trust (A.F.); the National Institutes of Health (grants R01CA120196 and R01CA129382 to A.F.; NCA CA21765 to SR and U24 CA114737 to E.P.), the Spanish Ministry of Science and Innovation (fellowship EX-2006-0739 to P.J.R.), a Canceropole Ile-de-France Research research grant (J.S.), the Eeastern Cooperative Oncology Group (ECOG) tumor bank and the European Organization for Research and Treatment of Cancer (EORTC) Children Leukemia Group, the Leukemia & Lymphoma Society Scholar Award (A.F.) and the Intramural Program of the US National Institutes of Health (P.D.A.). K. D. K. is a postdoctoral researcher funded by the "Fonds voor Wetenschappelijk Onderzoek-Vlaanderen" and recipient of a Belgian American Educational Foundation (BAEF) fellowship. D.A. is recipient of a predoctoral fellowship from the France National Cancer Institute (INCa). We are also grateful to T. Ludwig for helpful discussions and S. Cory (Walter and Eliza Hall Institute of Medical Research) and H.G. Wendel (Memorial Sloan Kettering Cancer Center) for the VavP-*Bcl2* mouse line

References

1. Ferrando AA, et al. Prognostic importance of TLX1 (HOX11) oncogene expression in adults with T-cell acute lymphoblastic leukaemia. Lancet. 2004; 363:535–536. [PubMed: 14975618]
2. Ferrando AA, et al. Gene expression signatures define novel oncogenic pathways in T cell acute lymphoblastic leukemia. Cancer Cell. 2002; 1:75–87. [PubMed: 12086890]
3. Kees UR, et al. Expression of HOX11 in childhood T-lineage acute lymphoblastic leukaemia can occur in the absence of cytogenetic aberration at 10q24: a study from the Children's Cancer Group (CCG). Leukemia. 2003; 17:887–893. [PubMed: 12750702]
4. Berger R, et al. t(5;14)/HOX11L2-positive T-cell acute lymphoblastic leukemia. A collaborative study of the Groupe Francais de Cytogenetique Hematologique (GFCH). Leukemia. 2003; 17:1851–1857. [PubMed: 12970786]
5. Bernard OA, et al. A new recurrent and specific cryptic translocation, t(5;14)(q35;q32), is associated with expression of the Hox11L2 gene in T acute lymphoblastic leukemia. Leukemia. 2001; 15 : 1495–1504. [PubMed: 11587205]
6. Bergeron J, et al. Prognostic and oncogenic relevance of TLX1/HOX11 expression level in TALLs. Blood. 2007; 110:2324–2330. [PubMed: 17609427]

7. Graux C, et al. Fusion of NUP214 to ABL1 on amplified episomes in T-cell acute lymphoblastic leukemia. Nat Genet. 2004; 36:1084–1089. [PubMed: 15361874]
8. Tosello V, et al. WT1 mutations in T-ALL. Blood. 2009; 114:1038–1045. [PubMed: 19494353]
9. Van Vlierberghe P, et al. PHF6 mutations in T-cell acute lymphoblastic leukemia. Nat Genet. 2010
10. Chaffin KE, et al. Dissection of thymocyte signaling pathways by in vivo expression of pertussis toxin ADP-ribosyltransferase. EMBO J. 1990; 9:3821–3829. [PubMed: 2123451]
11. Wildin RS, et al. Developmental regulation of lck gene expression in T lymphocytes. J Exp Med. 1991; 173:383–393. [PubMed: 1988541]
12. Gould J, Getz G, Monti S, Reich M, Mesirov JP. Comparative gene marker selection suite. Bioinformatics. 2006; 22:1924–1925. [PubMed: 16709585]
13. Weng AP, et al. Activating mutations of NOTCH1 in human T cell acute lymphoblastic leukemia. Science. 2004; 306:269–271. [PubMed: 15472075]
14. Sulis ML, et al. NOTCH1 extracellular juxtamembrane expansion mutations in T-ALL. Blood. 2008; 112:733–740. [PubMed: 18411416]
15. Palomero T, et al. Mutational loss of PTEN induces resistance to NOTCH1 inhibition in T-cell leukemia. Nat Med. 2007; 13:1203–1210. [PubMed: 17873882]
16. Maser RS, et al. Chromosomally unstable mouse tumours have genomic alterations similar to diverse human cancers. Nature. 2007; 447:966–971. [PubMed: 17515920]
17. Kawamura M, et al. Alterations of the p53, p21, p16, p15 and RAS genes in childhood T-cell acute lymphoblastic leukemia. Leuk Res. 1999; 23:115–126. [PubMed: 10071127]
18. Mullighan CG, et al. Genome-wide analysis of genetic alterations in acute lymphoblastic leukaemia. Nature. 2007; 446:758–764. [PubMed: 17344859]
19. Wakabayashi Y, et al. Bcl11b is required for differentiation and survival of alphabeta T lymphocytes. Nat Immunol. 2003; 4:533–539. [PubMed: 12717433]
20. Albu DI, et al. BCL11B is required for positive selection and survival of double-positive thymocytes. J Exp Med. 2007; 204:3003–3015. [PubMed: 17998389]
21. Hatano M, Roberts CW, Minden M, Crist WM, Korsmeyer SJ. Deregulation of a homeobox gene, HOX11, by the t(10;14) in T cell leukemia. Science. 1991; 253:79–82. [PubMed: 1676542]
22. Kawabe T, Muslin AJ, Korsmeyer SJ. HOX11 interacts with protein phosphatases PP2A and PP1 and disrupts a G2/M cell-cycle checkpoint. Nature. 1997; 385:454–458. [PubMed: 9009195]
23. Chen E, et al. Dysregulated expression of mitotic regulators is associated with B-cell lymphomagenesis in HOX11-transgenic mice. Oncogene. 2006; 25:2575–2587. [PubMed: 16407851]
24. Chandhok NS, Pellman D. A little CIN may cost a lot: revisiting aneuploidy and cancer. Curr Opin Genet Dev. 2009; 19:74–81. [PubMed: 19195877]
25. Margolin AA, et al. ChIP-on-chip significance analysis reveals large-scale binding and regulation by human transcription factor oncogenes. Proc Natl Acad Sci U S A. 2009; 106:244–249. [PubMed: 19118200]
26. Hebert J, Cayuela JM, Berkeley J, Sigaux F. Candidate tumor-suppressor genes MTS1 (p16INK4A) and MTS2 (p15INK4B) display frequent homozygous deletions in primary cells from T- but not from B-cell lineage acute lymphoblastic leukemias. Blood. 1994; 84:4038–4044. [PubMed: 7994022]
27. Kamimura K, et al. Haploinsufficiency of Bcl11b for suppression of lymphomagenesis and thymocyte development. Biochem Biophys Res Commun. 2007; 355:538–542. [PubMed: 17306224]
28. Ogilvy S, et al. Constitutive Bcl-2 expression throughout the hematopoietic compartment affects multiple lineages and enhances progenitor cell survival. Proc Natl Acad Sci U S A. 1999; 96:14943–14948. [PubMed: 10611317]
29. Egle A, Harris AW, Bath ML, O'Reilly L, Cory S. VavP-Bcl2 transgenic mice develop follicular lymphoma preceded by germinal center hyperplasia. Blood. 2004; 103:2276–2283. [PubMed: 14630790]
30. Li C, Wong WH. Model-based analysis of oligonucleotide arrays: expression index computation and outlier detection. Proc Natl Acad Sci U S A. 2001; 98:31–36. [PubMed: 11134512]

31. Reich M, et al. GenePattern 2.0. Nat Genet. 2006; 38:500–501. [PubMed: 16642009]
32. Van Vlierberghe P, et al. The recurrent SET-NUP214 fusion as a new HOXA activation mechanism in pediatric T-cell acute lymphoblastic leukemia. Blood. 2008; 111:4668–4680. [PubMed: 18299449]
33. Vilimas T, et al. Targeting the NF-kappaB signaling pathway in Notch1-induced T-cell leukemia. Nat Med. 2007; 13:70–77. [PubMed: 17173050]

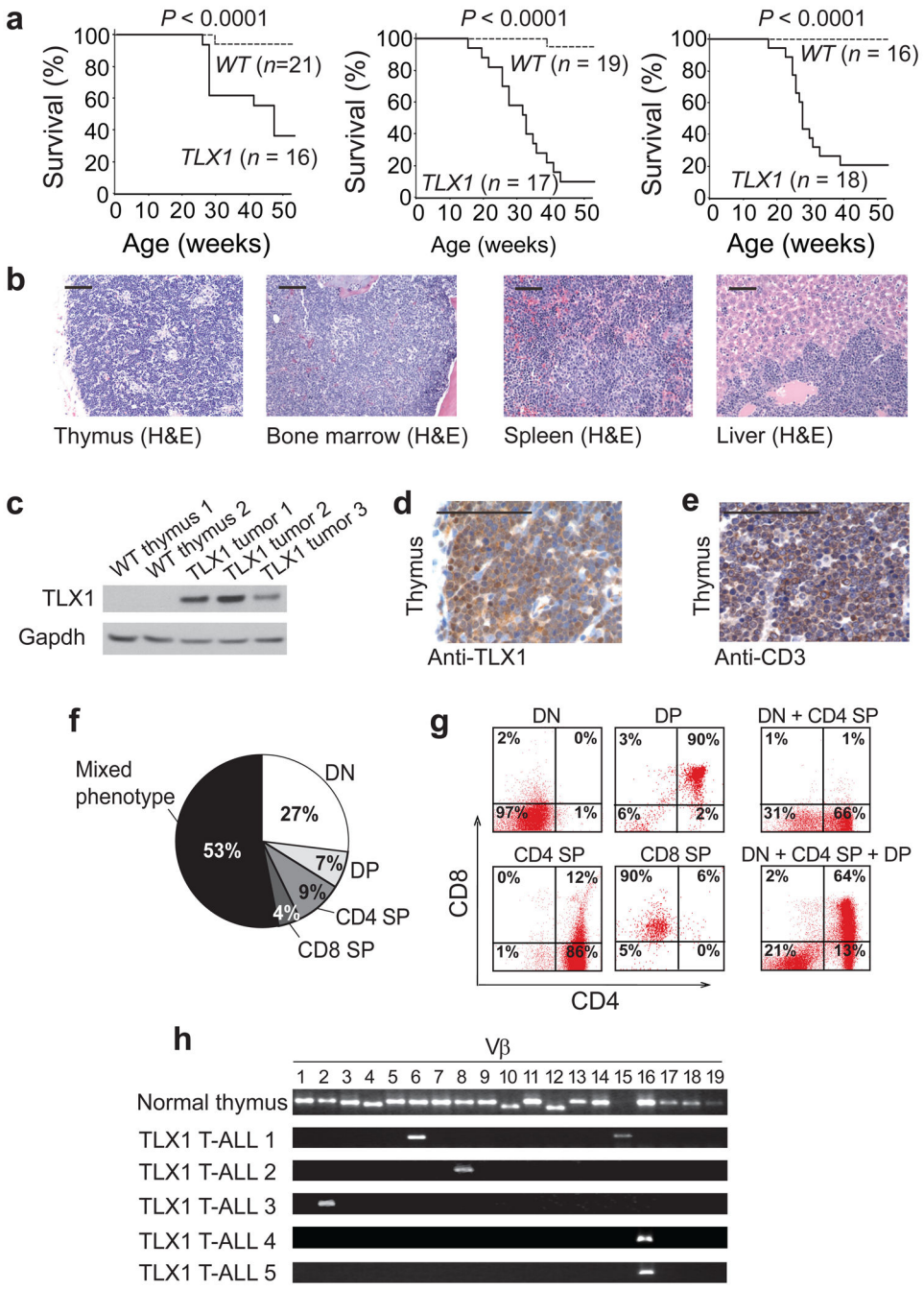

Fig. 1.

TLX1-induced T-cell leukemias in mice. (**a**) Kaplan-Meier survival curves of p56^{Lck}-*TLX1* transgenic mice and littermate controls from three independent founder lines. Accelerated mortality in *TLX1* transgenic mice was associated with the development of immature T-cell tumors. (**b**) Infiltration of thymus, spleen, bone marrow and liver by immature lymphoblasts. (**c**) Western blot analysis of TLX1 expression in mouse T-cell tumors. (**d-e**) Immunohistochemical analysis of *TLX1* (**d**) and CD3 expression in mouse *TLX1*-induced T-ALL cells (**e**). Scale bar 100 μm. (**f,g**) Immunophenotype distribution (**f**) and representative

flow cytometry plots (**g**) showing heterogeneous expression of CD4 and CD8 in *TLX1*-induced leukemias. DN, double negative; DP, double positive; SP, single positive. (**h**) Clonality analysis by expression of *TCRB* chains in *TLX1*-induced tumors. Polyclonal expression of *TCRB* in normal thymocytes is shown as control (upper row).

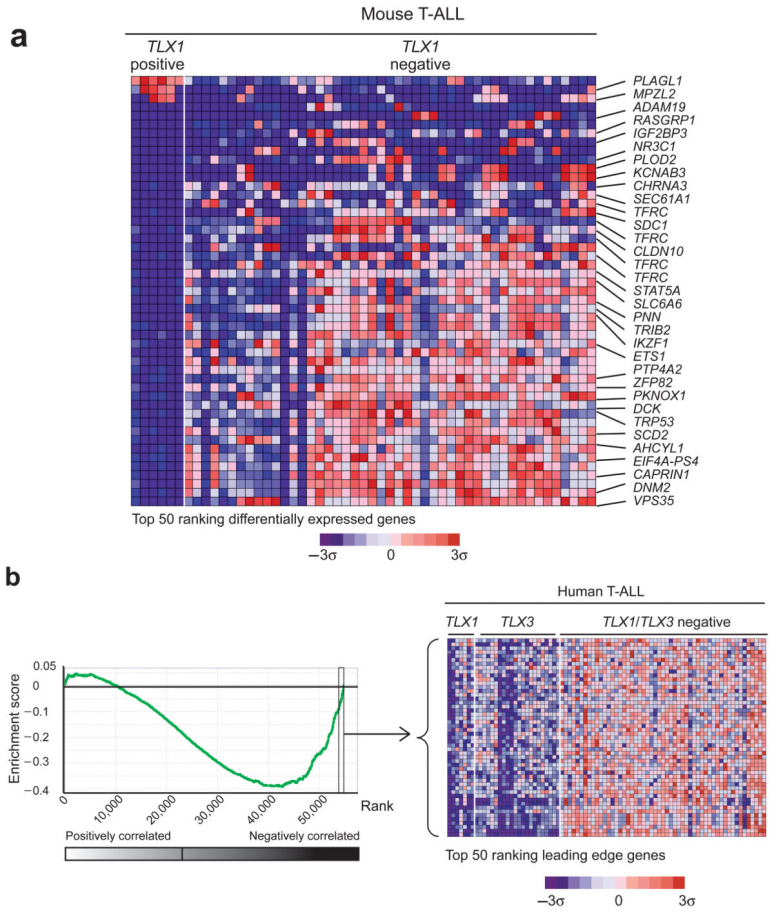

Fig. 2.

Molecular signatures associated with *TLX1*-induced transformation. (**a**) Heat map diagram of the 50 top ranking differentially expressed genes by *t*-test in mouse *TLX1*-induced leukemias. (**b**) GSEA analysis of differentially expressed genes associated with *TLX1*-induced transformation in mice demonstrates enrichment of this signature in human *TLX1*/*TLX3* expressing T-ALLs. Gene set: Human orthologs of mouse *TLX1* signature genes. Data set: *TLX1/TLX3* positive *vs. TLX1/TLX3* negative human leukemias. Enrichment plots (left) and heat map representations of the 50 top ranking genes in the leading edge (right) are shown. Genes in heat maps are shown in rows, each individual sample is shown in one column. The scale bar shows color coded differential expression from the mean in standard deviation units with red indicating higher levels and blue lower levels of expression.

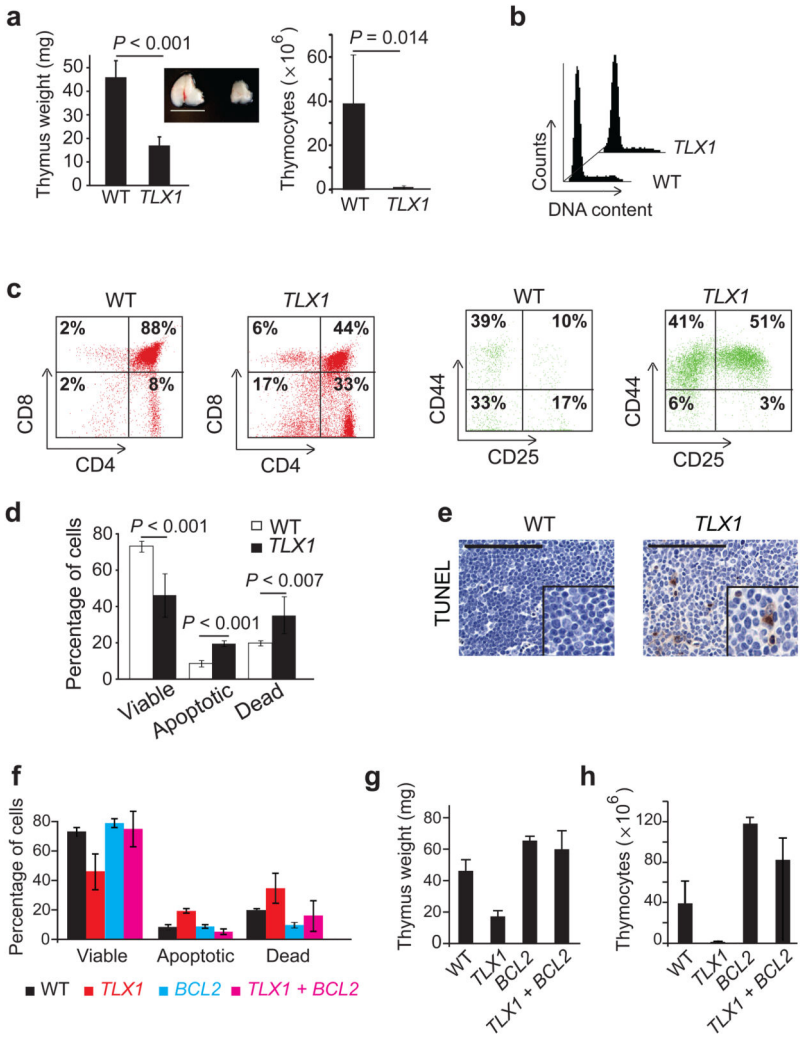

Fig 3. Developmental defects in thymocyte development in *TLX1*-transgenic mice

(**a**) Preleukemic *TLX1* transgenic mice at 6 weeks of age showed decreased thymus weight and cellularity compared with littermate controls. Scale bar 10 mm. (**b**) Cell cycle analysis of control and preleukemic *TLX1*-transgenic thymocytes via PI staining of DNA content analyzed by flow cytometry. (**c**) Flow cytometry analysis of T-cell development in preleukemic *TLX1*-transgenic animals. Accumulation of $CD44^{+}CD25^{+}$ cells shows a differentiation block at the DN2 stage of thymocyte development. (**d**) Apoptosis analysis of control and *TLX1*-transgenic preleukemic thymocytes via annexinV/PI staining. (**e**) TUNEL staining on thymus tissue sections. Scale bars represent 100 μm. (**f-h**) Transgenic expression of *BCL2* inhibits apoptosis (**f**) and reverses thymic weight (**g**) and cellularity (**h**) in preleukemic *TLX1 +BCL2* double transgenic mice.

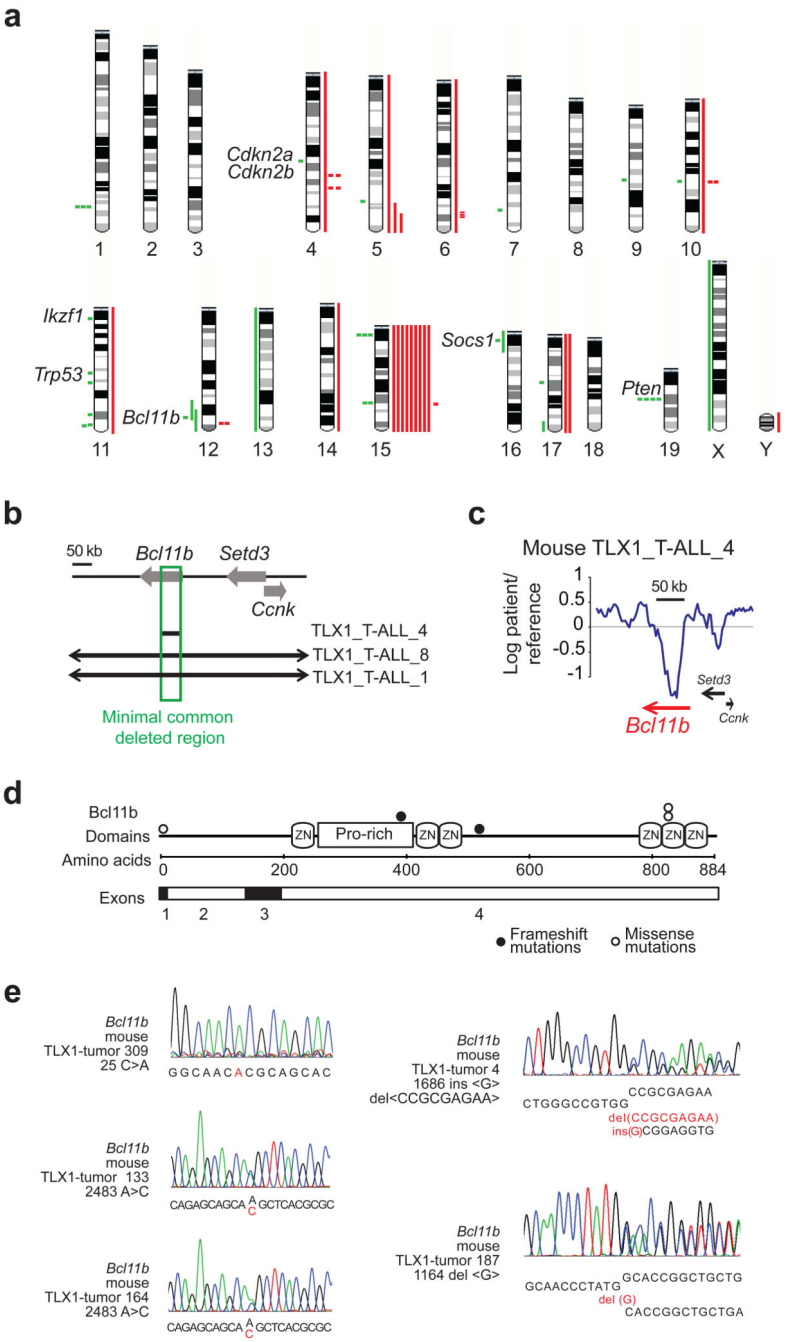

Fig. 4.

Numerical and structural chromosomal alterations in *TLX1*-induced mouse T-ALLs. (**a**) Mouse chromosomal ideogram showing the areas of genetic gain and loss identified by aCGH in *TLX1* thymic tumors. Red bars represent areas of gain. Green bars represent areas of copy number loss. (**b**) Schematic representation of the chromosome 12q commonly deleted region encompassing the *Bcl11b* locus in mouse *TLX1*-induced tumors. (**c**) Array CGH plot showing a focal deletion of the *Bcl11b* gene in a mouse *TLX1*-induced T-ALL. (**d**) Schematic representation of *Bcl11b* mutations identified in mouse *TLX1*-induced T-ALLs.

(**e**) DNA sequence chromatograms corresponding to *Bcl11b* mutations identified in mouse *TLX1*-induced T-ALLs.

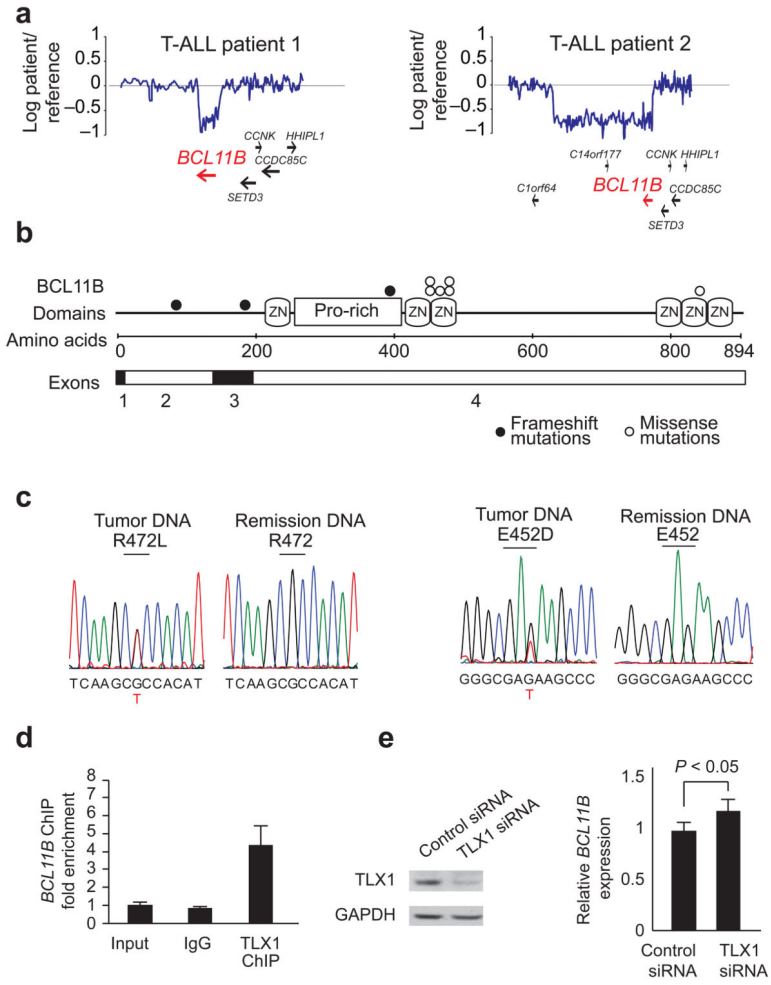

Fig. 5.

BCL11B is a TLX1 target gene mutated in human T-ALL. (**a**) Array CGH plots showing focal deletions in chromosomal band 14q32.2 encompassing the *BCL11B* locus in human T-ALL. (**b**) Schematic representation of *BCL11B* mutations identified in human T-ALL. (**c**) DNA sequence analysis of *BCL11B* in diagnostic and remission T-ALL samples. (**d**) ChIP analysis of TLX1 binding to *BCL11B* regulatory sequences in ALL-SIL cells. (**e**) Western blot analysis of TLX1 and RT-PCR analysis of *BCL11B* expression in ALL-SIL cells electroporated with control or *TLX1* siRNAs.

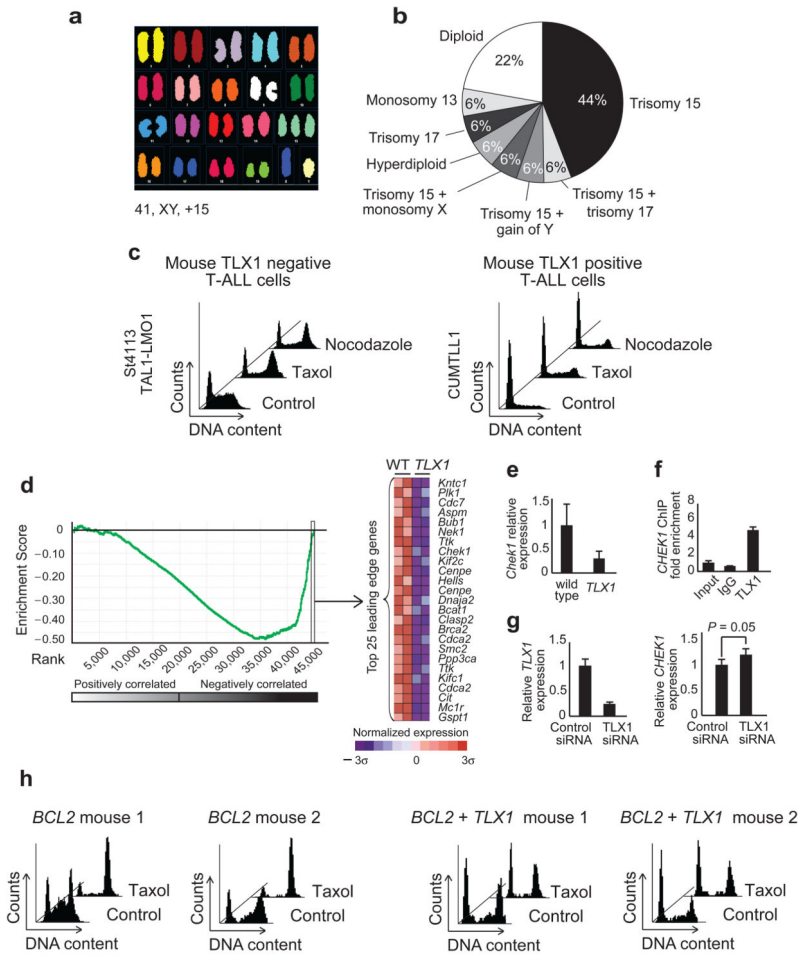

Fig. 6.

Numerical chromosomal alterations and defects in the mitotic checkpoint in *TLX*-transgenic mice. (**a**) SKY analysis of a mouse *TLX1*-induced tumor with trisomy 15. (**b**) Distribution of numerical chromosomal aberrations found by SKY and aCGH analysis in mouse *TLX1*-induced leukemias. (**c**) Cell cycle analysis of vehicle only, taxol and nocodazole treated mouse T-ALLs showing defective activation of the mitotic checkpoint in mouse *TLX1*-positive leukemia cells. (**d**) GSEA analysis of mitotic regulators identified as TLX1 direct target genes by ChIP-chip in sorted thymocytes (DN2 cells) from wild type and preleukemic *TLX1* transgenic mice. Gene set: TLX1 direct targets in mitotic cell cycle (GO:0000278). Data set: *TLX1* transgenic preleukemic cells *vs.* wild type. The enrichment plot (left) and heat map representation of the top 25 mitotic genes in the rank of transcripts differentially expressed in *TLX1*-preleukemic cells (right) are shown. The scale bar at the bottom shows color coded differential expression from the mean in standard deviation units with red indicating higher levels and blue lower levels of expression. (**e**) RT-PCR analysis of *Chek1* expression in thymocytes isolated from wild type or *TLX1*-transgenic mice. (**f**) ChIP analysis of TLX1 binding to *CHEK1* regulatory sequences in ALL-SIL cells. (**g**) RT-PCR analysis of *TLX1* and *CHEK1* expression in ALL-SIL cells electroporated with control or *TLX1* siRNAs. (**h**) Cell cycle analysis of vehicle only and taxol treated mouse thymocytes from

BCL2 transgenic and *TLX1-BCL2* double transgenic mice showing defective activation of the mitotic checkpoint in mouse *TLX1-BCL2*-expressing preleukemic cells.